

Low-energy dynamics of the $\gamma\gamma \rightarrow \pi\pi$ reaction in the NJL model¹

B. Bajc[†], A.H. Blin[§], B. Hiller[§], M.C. Nemes*,
A.A. Osipov[‡] and M. Rosina^{†X}

[†]Institut Jožef Stefan, Jamova 39, p.p.100, 61111 Ljubljana, Slovenia

[§]Centro de Física Teórica, Dpt. de Física, P-3000 Coimbra, Portugal

*Dpt. de Física, ICEX, Universidade Federal de Minas Gerais, C.P.702, 31270 Belo Horizonte-MG, Brasil

[‡]Joint Institute for Nuclear Research, Laboratory of Nuclear Problems, 141980 Dubna, Moscow Region, Russia

^XDpt. of Physics, University of Ljubljana, Jadranska 19, p.p. 64, 61111 Ljubljana, Slovenia

ABSTRACT

We calculate the one-quark-loop amplitude for the low energy $\gamma\gamma \rightarrow \pi\pi$ collision in the context of the Nambu and Jona-Lasinio model with scalar and pseudoscalar four quark couplings to all orders in the external momenta. We show that the NJL predictions for the $\gamma\gamma \rightarrow \pi^+\pi^-$ reaction are not far from the Born amplitude, which is close to the data, and is compatible with the chiral perturbation theory estimations. We determine the corrections given by the NJL model in leading order of $1/N_c$ to the chiral loop amplitude for $\gamma\gamma \rightarrow \pi^0\pi^0$. Numerical results for the $\gamma\gamma \rightarrow \pi\pi$ cross sections and for pion polarizabilities are given.

¹Work supported in part by CERN nos. - FAE/74/91 and - FIS/116/94, JNICT, CNPq, the Russian Foundation for Basic Research No 94-02-03028 and the Ministry of Science and Technology of the Republic of Slovenia.

1 Introduction

Currently there is much interest in calculations of the cross sections for the $\gamma\gamma \rightarrow \pi^+\pi^-$ and $\gamma\gamma \rightarrow \pi^0\pi^0$ modes. In [1] these processes were considered in the framework of chiral perturbation theory (CHPT) [2]-[4] in the next-to-leading order. Moderate enhancement for the $\pi^+\pi^-$ production near threshold and a small steadily rising cross section for the $\pi^0\pi^0$ production were shown. For the charged channel the chiral calculation [1] at the next-to-leading order is in good agreement with experimental data [5]. For the neutral channel the theoretical picture is more complicated. Tree diagrams are absent at the p^4 level for $\gamma\gamma \rightarrow \pi^0\pi^0$ which starts with meson-one-loop graphs. The one-loop result [1] for $\pi^0\pi^0$ production deviates from the Crystal Ball data [6] by 25-30% in the amplitude. Only the two-loop calculations (the p^6 order) [7] have reconciled CHPT with experiment and with dispersion calculations [8]-[10]. Three new constants d_i which appear at this order in the $L^{(6)}$ CHPT Lagrangian have been estimated with resonance saturation. At present it is impossible to determine d_i from other processes. This still leaves an uncertainty in the CHPT calculation.

Formerly [11] an attempt was made to estimate the tree-level contribution which starts at order p^6 for $\pi^0\pi^0$ production. Within specific models one can predict higher order constants of the effective meson Lagrangian at least at the tree level, i.e. to leading order in $1/N_c$. One can expect that tree-level contributions dominate over meson loops when they work at the same order in chiral counting. In this case, calculation of these tree-level contributions yields the main part of higher order corrections to the leading p^4 result for neutral pion production. Therefore there arises an opportunity not only to estimate the corrections appearing in the p^6 approximation but also to advance in energy. This yields indirect information on the convergence rate of the chiral series. Besides, it is not impossible that in some cases strong compensations of contributions from box diagrams on the one hand and from σ -exchange diagrams on the other can be observed in the p^6 approximation. If so, the contributions of the order of p^8 will be particularly important.

In this paper, following in general the main idea of [11] we calculate the leading $1/N_c$ contribution to $\gamma\gamma \rightarrow \pi\pi$ to *all orders in external momenta and quark masses*, in the context of the Nambu and Jona-Lasinio (NJL) model [12]. A small number of parameters is an obvious advantage of the model as compared with the resonance saturation method where the number of parameters increases when new transitions and higher chiral orders are considered. Mathematical tools allowing the higher terms of the chiral expansion to be calculated are provided by the momentum-space bosonization method [13]. It is clear that other known methods [14]-[18] would lead us to the same results. We consider the NJL Lagrangian only with pseudoscalar and scalar couplings. The vector and axial-vector contributions are beyond the scope of this paper². Also, the main bulk of events are peaked near on-shell values of the photons, so we present calculations only for real photons.

In the recently published papers [20] and [21] the NJL model is also used to investigate the process $\gamma\gamma \rightarrow \pi^0\pi^0$. In contrast to this, we consider not only the neutral mode but also the charged one $\gamma\gamma \rightarrow \pi^+\pi^-$. Besides, in the above papers the amplitude was

²We refer the readers to the papers [13] and [19] where the $\pi\pi$ -scattering amplitude has been calculated in the same framework using the NJL Lagrangian without spin-1 mesons and with them. The result clearly indicates only a small impact of a model extension like this on the final picture near threshold.

derived only to $\mathcal{O}(p^6)$ while we do not confine ourselves to this approximation. While analyzing the referee's comments on our work we learned of the results published in the preprint [22]. Its authors employed another method to take into account the total momentum dependence of meson vertices [18]. They managed to solve the problem only numerically. In our paper we derive *analytical* expressions for the amplitudes in question, with full momentum dependence, and formulae for pion polarizabilities. This allows us to construct chiral expansions of the amplitude and to investigate the role of the first p^6 and p^8 approximations.

The article is organized as follows. In Sec. 2 we set up the notation. In Sec. 3 we give a short description of the model and obtain general expressions for amplitudes of the $\gamma\gamma \rightarrow \pi\pi$ reaction. In Sec. 4 we consider the specific neutral mode $\gamma\gamma \rightarrow \pi^0\pi^0$, obtain the cross section for this process and calculate the polarizabilities of neutral pions. The same program is realized for the charged mode in Sec. 5. Finally, a summary and concluding remarks are presented in Sec. 6.

2 Kinematics

We consider the collision of two on-shell photons yielding two pions in the exit channel

$$\gamma(p_1, \epsilon_\mu) + \gamma(p_2, \epsilon_\nu) \rightarrow \pi^a(p_3) + \pi^b(p_4),$$

where a, b are the isotopic indices. The matrix element for pion production is

$$T(p_1, p_2, p_3) = e^2 \epsilon^\mu(p_1) \epsilon^\nu(p_2) T_{\mu\nu}(p_1, p_2, p_3), \quad (1)$$

where e is the electric charge.

One can decompose $T_{\mu\nu}$ into Lorentz and parity invariant amplitudes

$$T_{\mu\nu} = C_1 g_{\mu\nu} + C_2 p_{2\mu} p_{1\nu} + C_3 p_{2\mu} p_{3\nu} + C_4 p_{3\mu} p_{1\nu} + C_5 p_{3\mu} p_{3\nu} \quad (2)$$

where the terms proportional to $p_{1\mu}$ and $p_{2\nu}$ are not considered since they drop out when contracted with the polarization vectors in (1),

$$p_1^\mu \epsilon_\mu(p_1) = p_2^\nu \epsilon_\nu(p_2) = 0. \quad (3)$$

From the Ward identities

$$p_1^\mu T_{\mu\nu} = T_{\mu\nu} p_2^\nu = 0, \quad (4)$$

and the on-shell conditions $p_1^2 = p_2^2 = 0$, $p_3^2 = p_4^2 = m_\pi^2$ one gets the following constraints between the C_i

$$\begin{aligned} C_1 + C_2(p_1 p_2) + C_4(p_1 p_3) &= 0, & C_1 + C_2(p_1 p_2) + C_3(p_2 p_3) &= 0, \\ C_3(p_1 p_2) + C_5(p_1 p_3) &= 0, & C_4(p_1 p_2) + C_5(p_2 p_3) &= 0. \end{aligned} \quad (5)$$

Expressing all the scalar products $(p_i p_j)$ in terms of Mandelstam variables

$$s = (p_1 + p_2)^2, \quad t = (p_1 - p_3)^2, \quad u = (p_1 - p_4)^2, \quad s + t + u = 2m_\pi^2, \quad (6)$$

redefining $C_2 = A(s, t, u)$ and $C_5 = -sB(s, t, u)$, and with the following useful designations,

$$\xi_n = \xi - nm_\pi^2, \quad \xi = s, t, u, \quad Y = ut - m_\pi^4 = u_1 t_1 - sm_\pi^2, \quad (7)$$

one gets

$$T_{\mu\nu} = A(s, t, u)\mathcal{L}_{1\mu\nu} + B(s, t, u)\mathcal{L}_{2\mu\nu}, \quad (8)$$

with the gauge invariant tensors

$$\mathcal{L}_1^{\mu\nu} = p_2^\mu p_1^\nu - \frac{s}{2}g^{\mu\nu}, \quad (9)$$

$$\mathcal{L}_2^{\mu\nu} = -\left(\frac{u_1 t_1}{2}g^{\mu\nu} + t_1 p_2^\mu p_3^\nu + u_1 p_3^\mu p_1^\nu + s p_3^\mu p_3^\nu\right). \quad (10)$$

The amplitudes H_{++} (H_{+-}) with equal (opposite) helicity photons are

$$H_{++} = -(A + m_\pi^2 B), \quad H_{+-} = \frac{Y}{s}B. \quad (11)$$

The differential cross section for $\gamma\gamma \rightarrow \pi\pi$ with averaged photon polarizations in the center-of-mass system are calculated by the standard expression

$$\begin{aligned} \frac{d\sigma^{\gamma\gamma \rightarrow \pi\pi}}{d\Omega} &= \frac{\alpha^2 s}{32\mathcal{S}}\beta(s)H(s, t), \\ \beta(s) &= (1 - 4m_\pi^2/s)^{1/2}, \\ H(s, t) &= |H_{++}|^2 + |H_{+-}|^2. \end{aligned} \quad (12)$$

The factor \mathcal{S} is 1 (2) for $\pi^+\pi^-$ ($\pi^0\pi^0$). Let θ be the scattering angle in the center-of-mass system. To compare our results with experiment, the maximum value of the integration variable $(\cos\theta)_{\max}$ is equal to 0.6 for $\pi^+\pi^-$ [5] and 0.8 for $\pi^0\pi^0$ [6].

3 The model

3.1. The Lagrangian

The original SU(2) flavor NJL Lagrangian [12] with the fermionic degrees of freedom reinterpreted as the light up, u , and down, d , quarks incorporates the essential symmetries for the description of systems involving pions. We use it here in the form

$$\mathcal{L} = \bar{\psi}[i\partial - \mathcal{M} - eQA]\psi + \frac{G}{2}[(\bar{\psi}\psi)^2 + (\bar{\psi}i\gamma_5\tau_i\psi)^2], \quad (13)$$

where G is the strong coupling constant of the four-fermion interaction and \mathcal{M} is the diagonal current quark mass matrix explicitly breaking the chiral symmetry of the Lagrangian. We use $\hat{m}_u = \hat{m}_d = \hat{m}$ for the matrix elements of \mathcal{M} . The electromagnetic interactions are introduced by the replacement $\partial_\mu \rightarrow \partial_\mu + ieQA_\mu$, where $Q = (1 + 3\tau_3)/6$ is the charge matrix in the isotopic space.

Pions appear as the Goldstone modes associated with the spontaneous breaking of chiral symmetry. The constituent quark masses (m) are generated by the gap equation

$$m - \hat{m} = 8mGI_1. \quad (14)$$

We give all necessary definitions for quark-loop integrals I_i in the Appendix. We use the Pauli-Villars regularization [23]-[25], introducing one Pauli-Villars regulator in such a way [19], that the basic scalar integrals I_i coincide with those of the usual regularization scheme with a covariant four-momentum cutoff, Λ . In the following we shall refer to the quark one-loops of NJL as tree contributions (in terms of meson fields). To obtain the two-pion production amplitude on the basis of Lagrangian (13) one can use the momentum-space bosonization method [13] or any other [14]-[18]. Let us stress that we calculate the tree level contributions at all orders in p^2 , in leading $1/N_c$. In chiral perturbation theory this corresponds to the coefficients of the operators in the tree level Lagrangian to all orders in a momentum expansion.

The collective variables describing meson excitations are taken in the form of quark-antiquark field combinations linearly transformed with respect to the chiral group action. This method is completely equivalent to the existing nonlinear approaches but yields fewer Feynman diagrams in concrete calculations. We already discussed this issue in detail in [19].

3.2. The $\gamma\gamma \rightarrow \pi\pi$ amplitude in the NJL model

Our task is to calculate contributions from quark one-loop diagrams to the amplitudes $A(s, t, u)$ and $B(s, t, u)$ within the NJL model. Before going into detail, we make a few general comments. With the NJL model, one can calculate arbitrary N -point functions to all orders in external momenta. These calculations correspond to allowing for all tree contributions, i.e. terms leading in $1/N_c$. The next step is to examine one-loop meson diagrams [26]. However one has to confine oneself only to the first terms of the momentum expansion of the effective meson vertices derived from quark loops. Now it is not clear how to do it in a general case. Thus the following point of view seems reasonable. If there is a tree contribution, considering meson loop diagrams results in small corrections which can be ignored in the first approximation. And only if there is no tree contribution for whatever reason, consideration of meson loops is mandatory. This idea underlies for example the calculations in [11]. We shall follow it.

The process $\gamma\gamma \rightarrow \pi^+\pi^-$ is known to have tree contributions in all orders of the chiral expansion. It is these contributions that we shall calculate by the NJL model here. For the neutral $\gamma\gamma \rightarrow \pi^0\pi^0$ channel, tree contributions appear only in the p^6 and higher approximations. At a level of p^4 the amplitudes $A(s, t, u)$ and $B(s, t, u)$ are only determined by meson loop diagrams calculated in [1, 9]. This result does not depend on the model used and is of general character. We shall use it as a leading approximation³.

$$A_{c.l.}^N = -4 \frac{s - m_\pi^2}{sf^2} \bar{G}_\pi(s), \quad B_{c.l.}^N = 0. \quad (15)$$

³We ignore the kaon loop contribution, since we work in SU(2); its contribution is small in the kinematical region that we address [1].

Here f is the value of pion decay constant f_π in the chiral limit. The meson loop function $\bar{G}_\pi(s)$ is given in the Appendix⁴. We use the notation of [7] for the loop functions. Further, when describing the process, we shall calculate quark loop corrections to the leading contribution.

Let us turn to calculations. Contributing to the one-loop-order $\gamma\gamma \rightarrow \pi\pi$ amplitude in the NJL model are box diagrams of quarks, with two photons and two pions attached to the vertices, scalar exchange in the s -channel and pion exchange in the u and t channels. These diagrams are shown in fig.1. Pion exchange contributes only in the case of $\gamma\gamma \rightarrow \pi^+\pi^-$.

We proceed to calculate explicitly the contribution of the box diagrams, which is the most difficult to obtain. There are a total of six diagrams, with two distinct classes, one with photons being neighbors (four of this kind), see fig.1a, and the one with photons alternating with pions (two of this kind). The complete amplitude for the box diagrams, $T_{\mu\nu}^{(box)}$, is

$$\begin{aligned} T_{\mu\nu}^{(box)} &= 4g_\pi^2 Z_\pi^{-1} \left\{ f_1^{ab} [J_{\mu\nu}^{(1)}(p_1, p_1 + p_2, p_3) + J_{\mu\nu}^{(1)}(p_1, p_1 + p_2, p_4)] \right. \\ &\quad \left. + f_2^{ab} J_{\mu\nu}^{(2)}(p_1, p_1 - p_3, p_4) \right\}. \end{aligned} \quad (16)$$

Here g_π is the $\pi q\bar{q}$ coupling constant,

$$g_\pi^2 = \frac{1}{4I_2(m_\pi^2)}, \quad Z_\pi = 1 + \frac{m_\pi^2}{I_2(m_\pi^2)} \frac{\partial I_2(p^2)}{\partial p^2} \Big|_{p^2=m_\pi^2}. \quad (17)$$

The factors f_i^{ab} are the result of the trace over flavor. They are equal to

$$f_1^{ab} = \frac{10}{9}\delta_{ab}, \quad f_2^{ab} = \frac{2}{9}(9\delta_{a3}\delta_{b3} - 4\delta_{ab}). \quad (18)$$

As follows from these formulae, in the channels in question one has $f_1^N = f_2^N = f_1^C = 10/9$, $f_2^C = -8/9$, where we use the symbols N and C for the neutral and charged two-pion production respectively.

The Lorentz tensors $J_{\mu\nu}^{(i)}$ are the following two integrals, related to two topologically different box diagrams of fig.1a

$$J_{\mu\nu}^{(1)}(k_1, k_2, k_3) = \left(\frac{N_c}{4i}\right) \int_\Lambda \frac{d^4p}{(2\pi)^4} \text{Tr}[S(p)\gamma_\mu S(p+k_1)\gamma_\nu S(p+k_2)\gamma_5 S(p+k_3)\gamma_5], \quad (19)$$

and

$$\begin{aligned} J_{\mu\nu}^{(2)}(k_1, k_2, k_3) &= J_{\nu\mu}^{(2)}(k_3 - k_2, -k_2, k_1 - k_2) = \\ &= \left(\frac{N_c}{4i}\right) \int_\Lambda \frac{d^4p}{(2\pi)^4} \text{Tr}[S(p)\gamma_\mu S(p+k_1)\gamma_5 S(p+k_2)\gamma_\nu S(p+k_3)\gamma_5], \end{aligned} \quad (20)$$

where the standard notation is used,

$$S(p) = \frac{\not{p} + m}{p^2 - m^2}, \quad (21)$$

⁴The index π of the function $\bar{G}_\pi(s)$ indicates that this function differs from the function $\bar{G}(s)$ given in the Appendix only by having the pion mass in place of the quark mass.

and $N_c = 3$ is the number of colors. As a consequence of Furry's theorem, the following identities hold

$$J_{\mu\nu}^{(1)}(p_1, p_1 + p_2, p_3) = J_{\nu\mu}^{(1)}(p_2, p_1 + p_2, p_4), \quad (22)$$

$$J_{\mu\nu}^{(1)}(p_1, p_1 + p_2, p_4) = J_{\nu\mu}^{(1)}(p_2, p_1 + p_2, p_3), \quad (23)$$

$$J_{\mu\nu}^{(2)}(p_1, p_1 - p_3, p_4) = J_{\nu\mu}^{(2)}(p_2, p_2 - p_3, p_4). \quad (24)$$

These identities were used to obtain (16).

One can find that

$$\begin{aligned} & J_{\mu\nu}^{(1)}(p_1, p_1 + p_2, p_3) + J_{\mu\nu}^{(1)}(p_1, p_1 + p_2, p_4) = \\ & = \beta_{\mu\nu} - \frac{1}{s} \mathcal{L}_{1\mu\nu} \kappa_2(s, t, u) + \frac{1}{Y} \left(m_\pi^2 \mathcal{L}_{1\mu\nu} - \mathcal{L}_{2\mu\nu} \right) \kappa_3(s, t, u), \end{aligned} \quad (25)$$

$$\begin{aligned} & J_{\mu\nu}^{(2)}(p_1, p_1 - p_3, p_4) = \\ & = -\beta_{\mu\nu} + \frac{1}{s} \mathcal{L}_{1\mu\nu} \kappa_4(s, t, u) - \frac{(s - 2m_\pi^2)}{Y} \left(m_\pi^2 \mathcal{L}_{1\mu\nu} - \mathcal{L}_{2\mu\nu} \right) \kappa_5(s, t, u). \end{aligned} \quad (26)$$

Here we use the following notation

$$\begin{aligned} \beta^{\mu\nu} &= \frac{1}{2} g^{\mu\nu} \kappa_1(s, t, u) + (p_3^\mu p_3^\nu + p_4^\mu p_4^\nu) (\Delta_t I_2 + \Delta_u I_2) + \\ &+ \frac{1}{s} (s - 2m_\pi^2) (p_2^\mu p_3^\nu - p_3^\mu p_1^\nu) (\Delta_t I_2 - \Delta_u I_2), \end{aligned} \quad (27)$$

$$\Delta_\xi I_2 = \frac{1}{\xi_1} [I_2(\xi) - I_2(m_\pi^2)], \quad (28)$$

$$\kappa_1(s, t, u) = I_2(t) + I_2(u) + \frac{1}{s} (s - 2m_\pi^2) (u_1 \Delta_t I_2 + t_1 \Delta_u I_2), \quad (29)$$

$$\begin{aligned} \kappa_2(s, t, u) &= 3\tilde{Q}_3(s) + (s - 2m_\pi^2) [\Delta_t I_2 + \Delta_u I_2 + I_3(p_1, p_3) + I_3(p_2, p_3) - \\ &- Q_4(p_1, p_1 + p_2, p_3) - Q_4(p_1, p_1 + p_2, p_4)], \end{aligned} \quad (30)$$

$$\begin{aligned} \kappa_3(s, t, u) &= s I_3(p_1, -p_2) + t_1 I_3(p_1, p_3) + u_1 I_3(p_2, p_3) + (s - 2m_\pi^2) \kappa_6(s, t, u) - \\ &- \frac{s}{2} [t I_4(p_1, p_1 + p_2, p_3) + u I_4(p_1, p_1 + p_2, p_4)], \end{aligned} \quad (31)$$

$$\begin{aligned} \kappa_4(s, t, u) &= (s - 2m_\pi^2) [\Delta_t I_2 + \Delta_u I_2 + Q_4(p_1, p_1 - p_3, p_4) - I_3(p_2, p_3)] + \\ &+ \frac{2m_\pi^2}{s} \left[t_1 I_3(p_1, p_3) + u_1 I_3(p_2, p_3) - \frac{Y}{2} I_4(p_1, p_1 - p_3, p_4) \right], \end{aligned} \quad (32)$$

$$\kappa_5(s, t, u) = \frac{1}{s} [I_2(t) + I_2(u) - 2I_2(m_\pi^2)] + Q_4(p_1, p_1 - p_3, p_4) - I_3(p_2, p_3), \quad (33)$$

$$\begin{aligned} \kappa_6(s, t, u) &= \frac{1}{s} [I_2(t) + I_2(u) - 2I_2(m_\pi^2)] + I_3(p_3, -p_4) - Q_4(p_1, p_1 + p_2, p_3) - \\ &- Q_4(p_1, p_1 + p_2, p_4) - \frac{1}{2Y} \left\{ (s - 2m_\pi^2) [2t_1 I_3(p_1, p_3) + 2u_1 I_3(p_2, p_3) + \right. \\ &+ s I_3(p_1, -p_2) + s I_3(p_3, -p_4)] - 2m_\pi^2 [u_1 I_3(p_1, p_3) + t_1 I_3(p_2, p_3) + \\ &+ s I_3(p_3, -p_4)] + s [t^2 I_4(p_1, p_1 + p_2, p_3) + u^2 I_4(p_1, p_1 + p_2, p_4)] \left. \right\}. \end{aligned} \quad (34)$$

The rest of the notation is given in the Appendix. Note again that we systematically use the conditions (3) when deriving (25) and (26).

Now let us evaluate the scalar exchange, which contributes only to the s-channel, see fig.1b. Here one can obtain

$$T_{\mu\nu}^{(\sigma)} = 8g_\pi^2 Z_\pi^{-1} f_1^{ab} \mathcal{L}_{1\mu\nu} m^2 Q_3(s) \frac{[2I_2(s) + (s - 2m_\pi^2)I_3(p_3, -p_4)]}{\left[\frac{\hat{m}}{4mG} + (4m^2 - s)I_2(s)\right]}. \quad (35)$$

The function $Q_3(s)$ results from calculation of a triangular quark diagram describing two-photon decay of a scalar meson. It is given in the Appendix. The expression in the numerator is well known. It corresponds to the $\sigma\pi\pi$ vertex. The denominator stems from the scalar particle propagator. It is equal to $[m_\sigma^2(s) - s]/4g_\pi^2(s)$. The derived expression (35) is gauge-invariant.

Finally, we evaluate pion exchange, $T_{\mu\nu}^{(\pi)}$, which contributes to the t and u channels in the case of production of charged pions, see fig.1c. For on-shell photons we obtain

$$\begin{aligned} T_{\mu\nu}^{(\pi)} &= 8g_\pi^2 Z_\pi^{-1} (f_1^{ab} - f_2^{ab}) \left\{ \frac{p_{3\mu}(p_1 - p_3)_\nu}{t_1^2} [tI_2(t) - m_\pi^2 I_2(m_\pi^2)] + \right. \\ &\quad \left. + \frac{p_{3\nu}(p_2 - p_3)_\mu}{u_1^2} [uI_2(u) - m_\pi^2 I_2(m_\pi^2)] \right\}. \end{aligned} \quad (36)$$

In eq.(36) the pion propagator is cancelled by one of the $\gamma\pi\pi$ vertices.

The sum of (16) and (36) meets the general requirement of gauge invariance because it is proportional only to the Lorentz tensors $\mathcal{L}_1^{\mu\nu}$ and $\mathcal{L}_2^{\mu\nu}$

$$T_{\mu\nu}^{(box+\pi)} = 4g_\pi^2 Z_\pi^{-1} [f_1^{ab} R_{1\mu\nu} + f_2^{ab} R_{2\mu\nu}] \quad (37)$$

with

$$R_1^{\mu\nu} = 2\kappa_7 \mathcal{L}_2^{\mu\nu} - \frac{1}{s} \bar{\kappa}_2 \mathcal{L}_1^{\mu\nu} + \frac{1}{Y} (m_\pi^2 \mathcal{L}_1^{\mu\nu} - \mathcal{L}_2^{\mu\nu}) \kappa_3, \quad (38)$$

$$R_2^{\mu\nu} = -2\kappa_7 \mathcal{L}_2^{\mu\nu} + \frac{1}{s} \bar{\kappa}_4 \mathcal{L}_1^{\mu\nu} - \frac{1}{Y} (m_\pi^2 \mathcal{L}_1^{\mu\nu} - \mathcal{L}_2^{\mu\nu}) (s - 2m_\pi^2) \kappa_5. \quad (39)$$

Apart from the known functions $\kappa_i(s, t, u)$ (see (29)-(34)), we also use new ones

$$\kappa_7 = \frac{m_\pi^2}{s} \left[\frac{I_2(t)}{t_1^2} + \frac{I_2(u)}{u_1^2} \right] - \frac{I_2(m_\pi^2)}{u_1 t_1} \left[1 + \frac{m_\pi^2 (s - 2u_1 t_1)}{s t_1 u_1} \right], \quad (40)$$

$$\bar{\kappa}_2 = \kappa_2 - s(\Delta_t I_2 + \Delta_u I_2), \quad (41)$$

$$\bar{\kappa}_4 = \kappa_4 - s(\Delta_t I_2 + \Delta_u I_2). \quad (42)$$

Thus, we have all that is necessary for exploring physical consequences of the process under consideration. Before doing this, we point out that besides direct computation we also use another method for calculating amplitudes, namely projection of the sought-for amplitude $T_{\mu\nu}(s, t, u)$ by means of convolutions with tensors $\mathcal{L}_1^{\mu\nu}$ and $\mathcal{L}_2^{\mu\nu}$. A symbolic algebra program has been written for this purpose in REDUCE. First, the contributions to the amplitudes are calculated as functions of tensor integrals for all diagrams. Then the well known reduction method [27] is applied in order to transform the tensor integrals to a combination of a few basic scalar integrals (76)-(80). Finally, the amplitudes thus obtained are projected onto the gauge invariant tensors (9) and (10). The last step is necessary in order to have few compact and simple expressions, which are independent. This represents a consistency check for the methods used and in particular for the regularization scheme applied to the quark loop integrals.

4 The $\gamma\gamma \rightarrow \pi^0\pi^0$ mode

4.1. Chiral expansion of the amplitude

Theoretically of greatest interest is the neutral mode. Here the leading p^4 approximation is described by meson loops (see (15)). Yet, as was shown in the literature, this is not enough to describe the process quantitatively even in the near-threshold region. Let us elucidate the role of tree corrections. To this end, we isolate terms of order p^6 and p^8 from our general result. These terms are most important near the threshold. We start by expanding the amplitudes in a series of momenta. For box-type diagrams we get

$$T_{\mu\nu}^{(box)N} = \frac{40g_\pi^2}{9Z_\pi} \left\{ \mathcal{L}_{1\mu\nu} \left[-\frac{2}{3}I_3 + \left(m_\pi^2 - \frac{2s}{15} \right) I_4 + \left(\frac{2s^2}{7} - \frac{u_1 t_1}{2} + \frac{4m_\pi^4}{3} \right) I_5 \right] - \frac{1}{2} \mathcal{L}_{2\mu\nu} \left[I_4 - \left(\frac{s - 14m_\pi^2}{3} \right) I_5 \right] \right\} + \dots \quad (43)$$

where the superscript N stands for neutral channel. From here on we use the following notation

$$I_2 = I_2(0) = \frac{3}{16\pi^2} \left(\ln \frac{\Lambda^2 + m^2}{m^2} - \frac{\Lambda^2}{\Lambda^2 + m^2} \right), \quad (44)$$

$$I_3 = I_3(0) = -\frac{3h_1}{32\pi^2 m^2}, \quad h_1 = \left(\frac{\Lambda^2}{\Lambda^2 + m^2} \right)^2, \quad (45)$$

$$I_4 = I_4(0) = \frac{h_2}{32\pi^2 m^4}, \quad h_2 = \left(\frac{\Lambda^2 + 3m^2}{\Lambda^2 + m^2} \right) h_1, \quad (46)$$

$$I_5 = \frac{h_1(\Lambda^4 + 4\Lambda^2 m^2 + 6m^4)}{320\pi^2 m^6 (\Lambda^2 + m^2)^2}. \quad (47)$$

From the scalar exchange we have

$$T_{\mu\nu}^{(\sigma)N} = \frac{40g_\pi^2}{9Z_\pi} \mathcal{L}_{1\mu\nu} \left[\frac{2}{3}I_3 - \frac{7s}{60}I_4 + \frac{s - m_\pi^2}{6m^2}I_3 + \frac{s - 2m_\pi^2}{3I_2}I_3^2 + \frac{(s - m_\pi^2)^2}{24m^4}I_3 + \frac{3s^2 - 11sm_\pi^2 + 8m_\pi^4}{36m^2 I_2}I_3^2 + \frac{s(s - 2m_\pi^2)}{9I_2^2}I_3^3 - \frac{7s(s - m_\pi^2)}{240m^2}I_4 + \frac{40m_\pi^4 + 14sm_\pi^2 - 17s^2}{120I_2}I_3 I_4 - \frac{5s^2}{42}I_5 + \dots \right]. \quad (48)$$

As might be expected, by summing (43) and (48) the constant terms ($2I_3/3$) are cancelled (absence of tree contributions at a level of p^4), and others are grouped into a combination

$$T_{\mu\nu}^{(box+\sigma)N} = \frac{40g_\pi^2}{9Z_\pi} \left\{ \mathcal{L}_{1\mu\nu} \left[\frac{(s - m_\pi^2)}{6m^2} \left(1 + \frac{s - m_\pi^2}{4m^2} \right) I_3 - \frac{1}{4} \left(s - 4m_\pi^2 + \frac{7s(s - m_\pi^2)}{60m^2} \right) I_4 + \left(s - 2m_\pi^2 + \frac{3s^2 - 11sm_\pi^2 + 8m_\pi^4}{12m^2} \right) \frac{I_3^2}{3I_2} + \frac{s(s - 2m_\pi^2)}{9I_2^2}I_3^3 + \frac{40m_\pi^4 + 14sm_\pi^2 - 17s^2}{120I_2}I_3 I_4 + \frac{1}{6} \left(s^2 - 3u_1 t_1 + 8m_\pi^4 \right) I_5 \right] - \frac{1}{2} \mathcal{L}_{2\mu\nu} \left[I_4 - \left(\frac{s - 14m_\pi^2}{3} \right) I_5 \right] \right\} + \dots \quad (49)$$

Now let us switch to the chiral expansion of the obtained amplitude. This is an expansion in external momenta and masses of current quarks. We discussed the problem in detail within the NJL model in [19], where all necessary formulae can be found. The quantities corresponding to the leading terms of the chiral expansion will be labelled by an “o” above the respective symbol (except the chiral limit for the constant f_π traditionally designated by f). By algebraic transformations, we find (see (8)) for the amplitudes $A(s, t, u)$ and $B(s, t, u)$

$$\begin{aligned}
A^N(s, t, u) = & \frac{40\overset{\circ}{m}^2}{9f^2} \left\{ \frac{\overset{\circ}{I}_3}{6\overset{\circ}{m}^2} \left(s - \overset{\circ}{m}_\pi^2 + \frac{(s - 2\overset{\circ}{m}_\pi^2)^2}{4\overset{\circ}{m}^2} \right) + \frac{\overset{\circ}{I}_3}{3\overset{\circ}{I}_2} \left[(s - 2\overset{\circ}{m}_\pi^2) \left(1 - \frac{5\overset{\circ}{m}_\pi^2}{6\overset{\circ}{m}^2} \right) + \right. \right. \\
& + \left. \frac{s(s - 2\overset{\circ}{m}_\pi^2)}{4\overset{\circ}{m}^2} \right] - \frac{\overset{\circ}{I}_4}{4} \left[(s - 4\overset{\circ}{m}_\pi^2) \left(1 - \frac{3\overset{\circ}{m}^2\overset{\circ}{m}_\pi^2}{(\Lambda^2 + \overset{\circ}{m}^2)(\Lambda^2 + 3\overset{\circ}{m}^2)} \right) + \right. \\
& + \left. \frac{7s(s - \overset{\circ}{m}_\pi^2)}{60\overset{\circ}{m}^2} - \frac{2\overset{\circ}{m}_\pi^2(s - 3\overset{\circ}{m}_\pi^2)}{\overset{\circ}{m}^2} \right] + \frac{\overset{\circ}{I}_3^3}{9\overset{\circ}{I}_2^2} \left(s^2 - 6s\overset{\circ}{m}_\pi^2 + 12\overset{\circ}{m}_\pi^4 \right) + \\
& + \left. \frac{\overset{\circ}{I}_3\overset{\circ}{I}_4}{120\overset{\circ}{I}_2} \left[16\overset{\circ}{m}_\pi^2(9s - 20\overset{\circ}{m}_\pi^2) - 17s^2 \right] + \frac{\overset{\circ}{I}_5}{6} \left(s^2 - 3u_1t_1 + 8\overset{\circ}{m}_\pi^4 \right) \right\}, \quad (50)
\end{aligned}$$

$$B^N(s, t, u) = -\frac{20\overset{\circ}{m}^2\overset{\circ}{I}_4}{9f^2} \left[1 - \frac{\overset{\circ}{m}_\pi^2}{\overset{\circ}{m}^2} - \frac{3\overset{\circ}{m}^2\overset{\circ}{m}_\pi^2\overset{\circ}{h}_1}{\Lambda^4\overset{\circ}{h}_2} - \frac{\overset{\circ}{m}_\pi^2\overset{\circ}{I}_3}{3\overset{\circ}{I}_2} + \frac{14\overset{\circ}{m}_\pi^2 - s}{3\overset{\circ}{I}_4} \overset{\circ}{I}_5 \right]. \quad (51)$$

These expressions describe the tree-level contributions to the amplitudes $A^N(s, t, u)$ and $B^N(s, t, u)$, which involve terms of orders p^6 and p^8 . At $\Lambda \rightarrow \infty$ the term proportional to 1 in the amplitude $B^N(s, t, u)$ coincides with the expression derived in [11]. The terms of order p^6 in the amplitude $A^N(s, t, u)$ differ from the result of [11]. The discrepancy is due to the contribution from the σ meson exchange diagram, which was not considered there.

In the p^6 approximation the CHPT Lagrangian has three constants d_1 , d_2 and d_3 entering in the description of the process $\gamma\gamma \rightarrow \pi^0\pi^0$ [7]. In terms of d_i the amplitude of order p^6 in the process in question has the form

$$A^{(6)}(s, t, u) = -\frac{40}{9f^4} \left[(s - 2\overset{\circ}{m}_\pi^2)(4d_2 - d_1 - 8d_3) + 2(s - \overset{\circ}{m}_\pi^2)(d_1 + 4d_3) \right], \quad (52)$$

$$B^{(6)}(s, t, u) = \frac{80d_1}{9f^4}. \quad (53)$$

It is easy to see that the NJL model yields the following values for the constants

$$\begin{aligned}
d_1 &= -\frac{2f^2\overset{\circ}{h}_2}{(16\pi\overset{\circ}{m})^2} = -1.26 \times 10^{-4}, \\
d_2 &= \frac{f^2}{(16\pi\overset{\circ}{m})^2} \left[\overset{\circ}{h}_1 + \overset{\circ}{h}_2 - \frac{3\overset{\circ}{m}^2\overset{\circ}{h}_1}{(2\pi f)^2} \right] = 0.96 \times 10^{-4}, \\
d_3 &= \frac{f^2\overset{\circ}{h}_1}{2(16\pi\overset{\circ}{m})^2} = 2.89 \times 10^{-5}. \quad (54)
\end{aligned}$$

The analytical expressions for these coefficients fully agree with the corresponding expressions derived in [20], if one sets $g_A = 1$ there. For quantitative evaluation we used the numerical values of the model parameters fixed earlier in [13]: $\overset{\circ}{m} = 221.2$ MeV, $f = 88.6$ MeV, $\overset{\circ}{m}_\pi = 141.5$ MeV and $\Lambda = 1$ GeV. Note that these values correspond to the leading terms of the chiral expansion of the physical quantities chosen as follows: $m_\pi = 139$ MeV, $f_\pi = 93.1$ MeV, $m = 241.8$ MeV, $\Lambda = 1$ GeV.

An equivalent d_i -related set of parameters is also used. It includes constants a_1 , a_2 and b .

$$\begin{aligned}\frac{a_1}{(16\pi^2 f^2)^2} &= \left(\frac{20}{9f^4}\right) 16(d_3 - d_2), \\ \frac{a_2}{(16\pi^2 f^2)^2} &= \left(\frac{20}{9f^4}\right) (d_1 + 8d_2), \\ \frac{b}{(16\pi^2 f^2)^2} &= -\left(\frac{10}{9f^4}\right) d_1.\end{aligned}\tag{55}$$

The values we obtain for them are

$$\begin{aligned}a_1 &= \frac{10(4\pi f)^2}{9\overset{\circ}{m}^2} \left[\frac{3\overset{\circ}{m}^2 \overset{\circ}{h}_1^2}{2\pi^2 f^2} - \overset{\circ}{h}_1 - 2\overset{\circ}{h}_2 \right] = -59.5 \\ a_2 &= \frac{10(2\pi f)^2}{9\overset{\circ}{m}^2} \left[4\overset{\circ}{h}_1 + 3\overset{\circ}{h}_2 - \frac{3\overset{\circ}{m}^2 \overset{\circ}{h}_1^2}{\pi^2 f^2} \right] = 35.6 \\ b &= \frac{5(2\pi f)^2}{9\overset{\circ}{m}^2} \overset{\circ}{h}_2 = 3.5\end{aligned}\tag{56}$$

Let us compare these values with the results of [22], where the parameters a_1, a_2 and b were calculated within the extended NJL model.

$$\begin{aligned}a_1^{(ENJL)} &= -23.3, \\ a_2^{(ENJL)} &= 14.0, \\ b^{(ENJL)} &= 1.66.\end{aligned}\tag{57}$$

It is quite simple to account for the discrepancy. In the extended NJL model a_1, a_2 contain a factor $g_A^2 \simeq 0.37$ and b contains a factor $g_A \simeq 0.61$. This factor arises from allowing for vector mesons. In the NJL without vector mesons it is equal to 1. This is the reason for larger values of the parameters in (56). Yet, this does not mean that the NJL model without vector mesons cannot be used to describe the process in question qualitatively. This only indicates that chiral expansions in the NJL model converge slower than in the ENJL model, which we already know from [19]. Really, this means that if we want to compare the NJL result with the CHPT calculations, where chiral expansions converge quite fast, we must compare the *total* NJL result, which takes into account all orders of the chiral expansion. We shall return to this matter again when discussing numerical values of pion polarizabilities.

4.2. Polarizability of neutral pions

To obtain the pion polarizabilities we go to the crossed channel, Compton photon-pion scattering. This is easily done by trivial replacement of variables. The general expressions for the polarizabilities are obtained as

$$\beta_\pi^i = \frac{\alpha A^i}{2m_\pi} \Big|_{s,t_1,u_1=0} \quad (58)$$

$$(\alpha_\pi + \beta_\pi)^i = -\alpha m_\pi B^i \Big|_{s,t_1,u_1=0} \quad (59)$$

with $(i = N, C)$ and the coupling constant $\alpha = e^2/(4\pi) = 1/137$. In the case of charged pions, (C) calculated below in 5.2, the Born term is removed from the amplitudes. Different phase conventions are used in the literature. We adopt the one chosen in [7]. This is the Condon–Shortley phase convention. The one-loop result is

$$(\alpha_\pi + \beta_\pi)^N = 0, \quad (60)$$

$$(\alpha_\pi - \beta_\pi)^N = -\frac{\alpha}{48\pi^2 f^2 \dot{m}_\pi} = -1.0. \quad (61)$$

From here on we express the numerical values of polarizabilities in units 10^{-4} fm^3 . To this p^4 result one must add the p^6 and p^8 tree contributions obtained by us.

$$\begin{aligned} (\alpha_\pi + \beta_\pi)^N &= \frac{10\alpha \dot{m}_\pi}{(12\pi f \dot{m})^2} \left\{ \dot{h}_2 \left[1 - \frac{79\dot{m}_\pi^2}{120\dot{m}^2} - \frac{3\dot{m}^2 \dot{m}_\pi^2}{(\Lambda^2 + \dot{m}^2)(\Lambda^2 + 3\dot{m}^2)} \right] + \right. \\ &\quad \left. + \frac{\dot{m}_\pi^2 \dot{h}_1 \dot{h}_2}{(2\pi f)^2} + \frac{7\dot{m}^2 \dot{m}_\pi^2 \dot{h}_1}{5(\Lambda^2 + \dot{m}^2)^2} \right\} = 1.14 \end{aligned} \quad (62)$$

$$\begin{aligned} \beta_\pi^N &= \frac{5\alpha \dot{m}_\pi}{(12\pi f \dot{m})^2} \left\{ \dot{h}_1 \left(1 - \frac{7\dot{m}_\pi^2}{8\dot{m}^2} \right) - \frac{3\dot{m}^2 \dot{h}_1}{2\pi^2 f^2} \left(1 - \frac{5\dot{m}_\pi^2}{8\dot{m}^2} \right) + \right. \\ &\quad + 2\dot{h}_2 \left[1 - \frac{11\dot{m}_\pi^2}{8\dot{m}^2} - \frac{3\dot{m}^2 \dot{m}_\pi^2}{(\Lambda^2 + \dot{m}^2)(\Lambda^2 + 3\dot{m}^2)} \right] - \frac{15\dot{m}_\pi^2 \dot{m}^2 \dot{h}_1}{(2\pi f)^4} + \\ &\quad \left. + \frac{7\dot{m}_\pi^2 \dot{h}_1 \dot{h}_2}{(2\pi f)^2} + \frac{4\dot{m}_\pi^2 \dot{h}_1 (\Lambda^4 + 4\Lambda^2 \dot{m}^2 + 6\dot{m}^4)}{15\dot{m}^2 (\Lambda^2 + \dot{m}^2)^2} \right\} = 0.92 \end{aligned} \quad (63)$$

The numerical evaluation results are given in Table 1. It is evident from the table how important it is to calculate polarizabilities of neutral pions with allowance made for *all* terms of the chiral series and not only for its first terms. This can be most clearly demonstrated by examining the sum and the difference of polarizabilities. The pion loop is known not to contribute to the sum $(\alpha_\pi + \beta_\pi)$. In other words, this quantity stems only from many-loop contributions (meson two-loop, three-loop contributions, etc.,).

$$(\alpha_\pi + \beta_\pi)_{CHPT}^N = \sum_{n=2}^{\infty} S_{(n)} = \frac{8\alpha \dot{m}_\pi}{(4\pi f)^4} \sum_{n=2}^{\infty} s_{(n)}, \quad (64)$$

where the index n denotes a contribution from n -loop meson diagrams. The quantity $s_{(n)}$ is a sum of the contact contribution $s_{(n)}^r$ ($s_{(2)}^r = b^r = h_-^r$ in terms of notation from [7]) and the proper loop contribution $s_{(n)}^{(loops)}$:

$$s_{(n)} = s_{(n)}^r + s_{(n)}^{(loops)}. \quad (65)$$

Table 1: Neutral pion polarizabilities in the NJL model in units of 10^{-4} fm^3 . The results are compared with CHPT.

	1 loop	tree			total	CHPT [7]
		p^6	p^8	all others		
$(\alpha_\pi + \beta_\pi)^N$	0	1.44	-0.30	0.05	1.19	1.17 ± 0.30
$(\alpha_\pi - \beta_\pi)^N$	-1.0	-1.63	0.92	-0.45	-2.16	-1.90 ± 0.20
α_π^N	-0.5	-0.09	0.31	-0.20	-0.48	-0.35 ± 0.10
β_π^N	0.5	1.54	-0.62	0.25	1.67	1.50 ± 0.20

In [7] they calculated the first term of (64) $S_{(2)} = 1.0 + 0.17$. As in (65), here the first term corresponds to the contact contribution and the second term to the loop contribution. The total tree contribution, which is calculated in the NJL model, corresponds to the sum of the contact terms in a similar CHPT calculation. For the sum of polarizabilities of neutral pions we obtain the value

$$(\alpha_\pi + \beta_\pi)_{NJL}^N = 1.19 \sim \sum_{n=2}^{\infty} S_{(n)}^r. \quad (66)$$

Hence it can be concluded that the resonance saturation hypothesis, which is used to determine the contact contributions in CHPT and results, among other things in $S_{(2)}^r = 1.0$, holds good here because it leads, as it must, to fast convergence of the CHPT chiral series. It follows from our analysis that the sum of all other terms of this series accounts for only 20% of the leading contribution. Unlike the CHPT, where already the first term of the chiral series practically determines the entire result, the NJL model without vector mesons allows this at the second step. Moreover, if we confine ourselves to the first two terms of the chiral series in calculation of pion polarizabilities by the NJL model, we shall *fully* reproduce the picture we have in the CHPT with a_1^r and b^r fixed in conformity with the resonance saturation hypothesis. The parameter a_2^r is not associated with the pion polarizability, so we cannot get any more severe constraints on its value as compared with the already known ENJL result.

An interesting picture emerges for the difference of polarizabilities $(\alpha_\pi - \beta_\pi)$. Here we have

$$(\alpha_\pi - \beta_\pi)_{CHPT}^N = \sum_{n=1}^{\infty} D_{(n)} = \frac{8\alpha \mathring{m}_\pi}{(4\pi f)^4} \sum_{n=1}^{\infty} d_{(n)}. \quad (67)$$

As in (64), the quantity $d_{(n)}$ is a sum of the contact contribution $d_{(n)}^r$ ($d_{(2)}^r = a_1^r + 8b^r = h_+^r$ in terms of notation from [7]) and the proper loop contribution $d_{(n)}^{(loops)}$. In [7] they obtained $D_{(2)}^r = -0.58$ and $D_{(2)}^{(loops)} = -0.31$. In the NJL model, if we again confine ourselves to the sum of the first two terms of the chiral series, we get a close value $[(D_{(2)}^r) + (D_{(3)}^r)]_{NJL} = -0.70 \sim (D_{(2)}^r)_{CHPT}$. However it is evident from Table 1 that the chiral series of the NJL model for the difference of polarizabilities $(\alpha_\pi - \beta_\pi)$ converges noticeably worse. In this case we get

$$(\alpha_\pi - \beta_\pi)_{NJL}^N = -1.16 \sim \sum_{n=2}^{\infty} D_{(n)}^r, \quad (68)$$

which is twice as large (in absolute value) as the leading $(D_{(2)}^r)$ result of the CHPT. Hence it follows that in this case the resonance saturation hypothesis is less successful. This is

no surprise. The dispersion calculation methods leading to the sum rule for $(\alpha_\pi + \beta_\pi)$ are known to yield quite an exact result for this quantity. This is not the case with the difference $(\alpha_\pi - \beta_\pi)$ which features uncertainties in determination of the asymptotic contribution [28]. It is in these cases that the complete NJL model calculations are of particular interest. As we have just shown, they allow quite concrete conclusions to be drawn about the efficiency of the approximations used.

Let us also stress that the correction to the electric polarizability α_π^N at order p^6 is very small owing to strong compensation of the terms related to σ exchange (see the expression in parentheses)

$$\Delta^{(p^6)}\alpha_\pi^N = \frac{5\alpha\mathring{m}_\pi\mathring{h}_1}{(12\pi f\mathring{m})^2} \left(\frac{3\mathring{m}^2\mathring{h}_1}{2\pi^2 f^2} - 1 \right) = -0.09. \quad (69)$$

Therefore p^8 and higher order terms turn out to be essential here. Our calculations show that the contribution of these terms compensates almost fully the p^6 result. It indicates that the two-loop meson graphs are important for this value.

The process $\gamma\gamma \rightarrow \pi^0\pi^0$ has been used to obtain information on the polarizabilities. We give here the results obtained from the Crystal Ball data by Kaloshin, Persikov and Serebryakov.

$$\begin{aligned} (\alpha_\pi + \beta_\pi)^N &= 1.14 \pm 0.08 \pm 0.16, \quad [29] \\ (\alpha_\pi - \beta_\pi)^N &= -1.1 \pm 1.7. \quad [10] \end{aligned}$$

4.3. Interaction cross section

Before showing the results, we need to explain the parameters used. The values of the parameters m , f_π , m_π change at each order of the chiral expansion, but can always be expressed in terms of the leading chiral ones, \mathring{m} , f , \mathring{m}_π [19], which has been done in expressions (51)-(51) and in equations (71)-(72) below. The Mandelstam variables are always constrained by $s + t + u = 0$ and since the pion mass changes order by order, so does also the kinematically allowed region for s, t and u . For that reason the pion mass which appears in the polarization tensors $\mathcal{L}_1^{\mu\nu}$ and $\mathcal{L}_2^{\mu\nu}$ is the one calculated at a specific order. The same is true also for the phase space factor (12). In this way we get the same result by summing an infinite series of the chiral expansion or calculating the full amplitude. The pion loop has been calculated only at leading order and we have to take the pion mass of the specific tree order to which it is added. In Fig. 2 we display the data for the cross section $\sigma(s, |\cos\theta| \leq 0.8)$ as determined by the Crystal Ball collaboration [6]. They are shown as a function of the center-of-mass energy $W = \sqrt{s}$. The dotted line is a well-known result arising from consideration of the leading pion loop (15). The dot-and-dash line is the result at which we arrive on taking into account p^6 terms. The dashed line shows the data derived from the previous curve by including order p^8 corrections (51)-(51). The solid line shows the full result. The tree contributions are clearly seen to be responsible for enhancement of the scattering cross section in the near-threshold region, the tree p^6 approximation accounting for almost the entire effect. Diagrams with σ exchange dominate among the diagrams contributing to this result. Consideration of higher-order tree corrections practically do not affect the cross section in the low-energy region. The different thresholds correspond to the different values of the pion mass at a certain order of the chiral expansion.

5 The $\gamma\gamma \rightarrow \pi^+\pi^-$ mode

5.1. The result up to p^4

Let us begin with the leading-order result. Here the NJL model yields

$$A^C = -\frac{\overset{\circ}{h}_1}{(2\pi f)^2} + \dots, \quad B^C = -\frac{4}{u_1 t_1} + \dots \quad (70)$$

The ellipses indicate higher contributions. The amplitude resulting from insertion of B^C in (8) is the Born term and of order p^2 . The term A^C leads to the p^4 correction of the amplitude. Our task is to calculate corrections to these expressions arising from consideration of NJL tree diagrams. They can be derived from the general result given in Sec. 3. Here we shall dwell upon the role of the p^6 and p^8 corrections which account for the major part of the additional contribution.

5.2. The result up to p^6 and higher orders in the NJL model

Let us examine corrections to the leading terms of the chiral expansion of the $\gamma\gamma \rightarrow \pi^+\pi^-$ amplitude. Here we have

$$A^C(s, t, u) = \frac{8\overset{\circ}{m}^2}{3f^2} \overset{\circ}{I}_3 \left\{ 1 + \frac{5(s - \overset{\circ}{m}_\pi^2)}{18\overset{\circ}{m}^2} - \frac{\overset{\circ}{m}_\pi^2}{2\overset{\circ}{m}^2} \left(\frac{\Lambda^2 + 3\overset{\circ}{m}^2}{\Lambda^2 + \overset{\circ}{m}^2} \right) + \right. \\ \left. + \frac{\overset{\circ}{I}_3}{9\overset{\circ}{I}_2} (5s - 13\overset{\circ}{m}_\pi^2) + \frac{\overset{\circ}{I}_4}{6\overset{\circ}{I}_3} \left(\overset{\circ}{m}_\pi^2 - \frac{7s}{10} \right) \right\}, \quad (71)$$

$$B^C(s, t, u) = - \left\{ \frac{4}{u_1 t_1} \left[1 + \frac{1}{2} \left(\frac{3\overset{\circ}{m}_\pi^2 \overset{\circ}{h}_1}{8\pi^2 f^2} \right)^2 \right] + \frac{7\overset{\circ}{h}_2}{10(6\pi f \overset{\circ}{m})^2} \right\}. \quad (72)$$

One obtains the polarizabilities for the charged pions from equations (58) and (59) but with the Born term removed from the amplitude. We derive the p^4 and p^6 orders to the polarizabilities of charged pions to be

$$\beta_\pi^C = -\frac{2\alpha \overset{\circ}{h}_1}{\overset{\circ}{m}_\pi (4\pi f)^2} \left\{ 1 - \frac{5\overset{\circ}{m}_\pi^2}{18\overset{\circ}{m}^2} \left[\frac{11}{20} + 2 \left(\frac{\Lambda^2 + 3\overset{\circ}{m}^2}{\Lambda^2 + \overset{\circ}{m}^2} \right) - \frac{3\overset{\circ}{m}^2 \overset{\circ}{h}_1}{2\pi^2 f^2} \right] \right\} = -4.57, \quad (73)$$

$$(\alpha_\pi + \beta_\pi)^C = \frac{7\alpha \overset{\circ}{m}_\pi \overset{\circ}{h}_2}{10(6\pi f \overset{\circ}{m})^2} = 0.41. \quad (74)$$

Generally, it is these contributions that determine the amount of the electric and magnetic polarizabilities of charged pions. Table 2 presents numerical evaluation results for the polarizabilities. We also included corrections from p^8 terms in the table. Analytical expressions are quite cumbersome, so we do not show the whole of them. An exception is the sum $(\alpha_\pi + \beta_\pi)^C$, for which the order p^6 contribution is a leading one and the first correction at order p^8 amounts to 25%. The NJL model yields for it

$$(\alpha_\pi + \beta_\pi)^C = \frac{7\alpha \overset{\circ}{m}_\pi \overset{\circ}{h}_2}{10(6\pi f \overset{\circ}{m})^2} \left\{ 1 - \frac{125\overset{\circ}{m}_\pi^2}{168\overset{\circ}{m}^2} + \frac{\overset{\circ}{m}_\pi^2 \overset{\circ}{h}_1}{(2\pi f)^2} - \frac{13\overset{\circ}{m}^2 \overset{\circ}{m}_\pi^2 \overset{\circ}{h}_1}{7\Lambda^4 \overset{\circ}{h}_2} \right\} = 0.31. \quad (75)$$

Table 2: The charged pion polarizabilities in the NJL model in units of 10^{-4} fm^3 . The results are compared with phenomenological data.

	tree				total	exp.
	p^4	p^6	p^8	all others		
$(\alpha_\pi + \beta_\pi)^C$	0	0.41	-0.10	0.02	0.33	$1.4 \pm 3.1 \pm 2.5$ [31] $0.33 \pm 0.06 \pm 0.01$ [29] $0.22 \pm 0.07 \pm 0.04$ [29]
$(\alpha_\pi - \beta_\pi)^C$	11.62	-2.07	0.82	-0.36	10.0	$15.6 \pm 6.4 \pm 4.4$ [31] 4.8 ± 1.0 [10]
α_π^C	5.81	-0.83	0.36	-0.17	5.17	
β_π^C	-5.81	1.24	-0.46	0.19	-4.84	

Apart from the known results obtained in Serpukhov [31] from the reaction $\pi^- A \rightarrow \pi^- \gamma A$, the experimental body of the table incorporates the results of analyzing angular distributions of pions in the reaction $\gamma\gamma \rightarrow \pi^+\pi^-$ (CELLO and MARK-II data) within the framework of the unitary model for helicity 2 amplitude [29]. As seen from Table 2, the results of numerical calculations agree with the available experimental data. The electric and magnetic polarizabilities are mainly determined already at order p^4 . Only the sum of these quantities, which equals zero at this order, is determined by higher p^6 and p^8 corrections.

5.3. The amplitudes: numerical results

Let us turn to the diagrams illustrating the general formulae derived earlier. Figure 3 displays the charged pion production cross section as a function of energy in the center-of-mass system of interacting particles. Integration over the scattering angle covers the interval $|\cos\theta| < 0.6$. We show four curves. The dotted curve corresponds to the Born term derived from B^C in formula (70). Taking into account corrections up to p^4 , (70) and up to p^6 (see formulae in (71)-(72)) we get the dot-and-dash and the dashed curves respectively. Full calculations are represented by the solid curve. As was expected, the cross section for production of charged pion pairs features some enhancement caused by p^6 terms. The total result is close to p^6 estimations, in the low energy range. For higher values of the energy the scalar resonance starts to show up in the higher orders in momenta and in the full result.⁵

6 Conclusions

To summarize, we have calculated the quark one-loop contributions to the $\gamma\gamma \rightarrow \pi\pi$ processes, using the SU(2) flavor NJL model, with scalar-isoscalar and pseudoscalar-

⁵This behavior differs from the result obtained in [30], where the scalar resonance was hidden. This difference is a consequence of the different regularization schemes used. In order to have the right low energy behavior in the Compton photon-pion processes considered here one has to use Pauli-Villars regularization.

isovector four-quark interactions. These calculations correspond to full consideration of tree contributions in the examination of the above processes. We present the amplitudes in a compact and analytical form which is used to compute the associated cross sections and the polarizabilities of pions.

The chiral expansion of the $\gamma\gamma \rightarrow \pi^0\pi^0$ amplitude starts with p^4 terms. There are no tree contributions in this approximation, therefore the leading contribution is that from one-loop pion diagrams. We calculated the highest tree corrections appearing at order p^6 and showed that in the near-threshold region the cross section for this process can be satisfactorily described by one-loop pion diagrams (the p^4 order) with the tree p^6 contribution. The conclusion as to the smallness of the highest contributions (beginning with p^8 terms) to the cross section of the process under study in its near-threshold region is of interest to us. It is this kind of evaluation that the quark models are well suited for. For example, careful examination of this problem within the CHPT at order p^8 alone would require complicated calculations of the three-loop meson diagrams.

The NJL model predicts some enhancement of the cross section for $\gamma\gamma \rightarrow \pi^+\pi^-$ near threshold. This fact is in good agreement with the known CHPT result [1]. The increase of the cross sections in the full result for higher energies is an artifact of the model. This is why we have plotted them only for $W < 0.4$ GeV. One has to stay below the two constituent quark threshold where the lack of confinement in the NJL model starts dominating the result. Near the threshold this effect is absent and allows for extraction of the polarizabilities at *all* tree orders.

We show that to describe the cross sections well it is enough to consider only the first terms in a chiral expansion. Higher orders are important for polarizabilities. Therefore one can arrive at the general conclusion that the cross sections are very little sensitive to the polarizability. The same conclusion has been drawn in [9] in the framework of a dispersive approach. Among new interesting results are also calculations of the sum of the electric and magnetic polarizabilities presented here both for neutral and charged pions. At the one-loop meson order they are equal to zero, that is why it is very important to advance to higher $\sim p^8$ orders. This is possible with the NJL model, as we have shown here.

Appendix. The main loop integrals

List of the main quark-loop integrals

$$I_1 = iN_c \int_{\Lambda} \frac{d^4k}{(2\pi)^4} \Delta(k), \quad (76)$$

$$I_2(q_1) = -iN_c \int_{\Lambda} \frac{d^4k}{(2\pi)^4} \Delta(k) \Delta(k + q_1), \quad (77)$$

$$I_3(q_1, q_2) = -iN_c \int_{\Lambda} \frac{d^4k}{(2\pi)^4} \Delta(k) \Delta(k + q_1) \Delta(k + q_2), \quad (78)$$

$$I_4(q_1, q_2, q_3) = -iN_c \int_{\Lambda} \frac{d^4k}{(2\pi)^4} \Delta(k) \Delta(k + q_1) \Delta(k + q_2) \Delta(k + q_3), \quad (79)$$

$$Q_4(q_1, q_2, q_3) = -iN_c \int_{\Lambda} \frac{d^4k}{(2\pi)^4} k^2 \Delta(k) \Delta(k + q_1) \Delta(k + q_2) \Delta(k + q_3). \quad (80)$$

Here the notation

$$\Delta(p) = \frac{1}{p^2 - m^2} \quad (81)$$

has been used. A sharp euclidean cutoff Λ is introduced for the scalar integrals I_i, Q_4 , and all the cutoff dependence of the amplitude $T_{\mu\nu}$ resides in these integrals.

We also use the standard notations for the loop functions $\bar{G}(s), \bar{G}_\Lambda(s), \bar{J}_\Lambda(s)$ [7]. They are analytic in the complex s -plane, cut along the positive real axis for $\text{Re}(s) \geq 4m^2$ and $\text{Re}(s) \geq 4(\Lambda^2 + m^2)$ respectively. At small s ,

$$\bar{G}(s) = \frac{1}{16\pi^2} \sum_{n=1}^{\infty} \left(\frac{s}{m^2} \right)^n \frac{(n!)^2}{(n+1)(2n+1)!} \quad (82)$$

$$\bar{G}_\Lambda(s) = \frac{1}{16\pi^2} \sum_{n=1}^{\infty} \left(\frac{s}{\Lambda^2 + m^2} \right)^n \frac{(n!)^2}{(n+1)(2n+1)!} \quad (83)$$

$$\bar{J}_\Lambda(s) = \frac{1}{16\pi^2} \sum_{n=1}^{\infty} \left(\frac{s}{\Lambda^2 + m^2} \right)^n \frac{(n!)^2}{n(2n+1)!}. \quad (84)$$

Besides, we shall need the function

$$Q_3(s) = I_3(p_1, -p_2) + \frac{N_c}{s} \tilde{Q}_3(s), \quad (85)$$

where

$$\tilde{Q}_3(s) = \frac{4\Lambda^2}{4(\Lambda^2 + m^2) - s} \left[\bar{J}_\Lambda(s) - \frac{s}{32\pi^2(\Lambda^2 + m^2)} \right] + 2 \left[\bar{G}(s) - \frac{m^2}{\Lambda^2 + m^2} \bar{G}_\Lambda(s) \right]. \quad (86)$$

References

- [1] J. Bijnens and F. Cornet, Nucl. Phys. B296 (1988) 557.
- [2] S. Weinberg, Physica A 96 (1979) 327.
- [3] J. Gasser and H. Leutwyler, Ann. Phys. (N.Y.) 158 (1984) 142.
- [4] J. Gasser and H. Leutwyler, Nucl. Phys. B250 (1985) 465.
- [5] Mark II Collab., J. Boyer et al., Phys. Rev. D42 (1990) 1350.
- [6] Crystal Ball Collab., H. Marsiske et al., Phys. Rev. D41 (1990) 3324.
- [7] S. Bellucci, J. Gasser and M.E. Sainio, Nucl. Phys. B423 (1994) 80.
- [8] D. Morgan and M.R. Pennington, Z. Phys. C48 (1990) 623; Phys. Lett. B272 (1991) 134.
- [9] J.F. Donoghue, B.R. Holstein and Y.C. Lin, Phys. Rev. D37 (1988) 2423.
J.F. Donoghue and B.R. Holstein, Phys. Rev. D48 (1993) 137.
- [10] A.E. Kaloshin, V.V. Serebryakov, Irkutsk preprint ISU-IAP.Th 93-03, (hep-ph/9306224).

- [11] J. Bijnens, S. Dawson and G. Valencia, Phys. Rev. D44 (1991) 3555.
- [12] Y. Nambu and J. Jona-Lasinio, Phys. Rev. 122 (1961) 345; 124 (1961) 246.
- [13] V. Bernard, A.A. Osipov and U.-G. Meißner, Phys. Lett. B285 (1992) 119.
- [14] V. Bernard, R.L. Jaffe and U.-G. Meißner, Nucl. Phys. B308 (1988) 753.
- [15] S. Klimt, M. Lutz, U. Vogl and W. Weise, Nucl. Phys. A516 (1990) 429; U. Vogl, M. Lutz and W. Weise, Nucl. Phys. A516 (1990) 469.
- [16] An extensive list of references is given in S. Klevansky, Rev. Mod. Phys. 64 (1992) 649.
- [17] J. Bijnens, C. Bruno and E.de Rafael, Nucl. Phys. B390 (1993) 501.
- [18] J. Bijnens, preprint NORDITA 95/10 N,P (hep-ph/9502335); J. Bijnens and J. Prades, Z.Phys. C64 (1994) 475.
- [19] V. Bernard, A.H. Blin, B. Hiller, Yu.P. Ivanov, A.A. Osipov and U.-G. Meißner, Preprint CRN 95-25, TK 95 18 (hep-ph/9506309) to appear in Annals of Physics (N.Y.) (1996).
- [20] S. Bellucci and C. Bruno, Nucl. Phys. B452 (1995) 626.
- [21] A. Bel'kov, A. Lanyov and S. Scherer, Preprint JINR-E2-95-266, hep-ph/9506406 (1995).
- [22] J. Bijnens, A. Fayyazuddin and J. Prades, preprint NORDITA - 95/84 N,P (hep-ph/9512374).
- [23] W. Pauli and F. Villars, Rev. Mod. Phys. 21 (1949) 434.
- [24] V. Bernard and D. Vautherin, Phys. Rev. D40 (1989) 1615.
- [25] C. Schüren, E.R. Arriola and K. Goeke, Nucl. Phys. A547 (1992) 612.
- [26] A. Blotz and K. Goeke, Int. J. Mod. Phys. A9 (1994) 2067; R. Lemmer and R. Tegen, "Meson cloud corrections to the pion electromagnetic form factor in the Nambu Jona-Lasinio model", Jülich preprint 1995.
- [27] G. Passarino and M. Veltman, Nucl. Phys. B160 (1979) 151.
- [28] V. A. Petrun'kin, Particles and Nuclei, Vol.12, Part 3 (1981) 692.
- [29] A.E. Kaloshin, V.M. Persikov and V.V. Serebryakov, Irkutsk preprint ISU-IAP.Th 95-01, (hep-ph/9504261).
- [30] B. Bajc, A.H. Blin, B. Hiller, M.C. Nemes and M. Rosina, Z. Phys. A350 (1994) 229.
- [31] Yu.M. Antipov et al., Z. Phys. C26 (1985) 495.

Figure captions

Fig.1 - Representative Feynman diagrams involved in the calculation of the amplitudes for $\gamma\gamma \rightarrow \pi\pi$, subject to permutations. a) Two photons (wiggled lines) and two pions (dashed lines) are directly coupled to the quarks (full lines). b) Quarks rescatter with the quantum numbers of a scalar-isoscalar, σ , in the s-channel. c) When a pair of charged pions is created, quarks can also rescatter in t- and u- channels to form an intermediate state with the quantum numbers of a pion.

Fig.2 - The NJL $\gamma\gamma \rightarrow \pi^0\pi^0$ cross section, with averaged photon polarizations, in comparison with the Crystal Ball data [6]. The dotted line results from the meson one-loop calculations (the p^4 order). The dash-dotted line includes up to p^6 tree level NJL corrections to the leading p^4 result. The dashed line takes into account up to p^8 tree order NJL corrections and the full line corresponds to the total tree order corrections of NJL to the pion loop.

Fig.3 - The NJL cross section for the $\gamma\gamma \rightarrow \pi^+\pi^-$ mode, with averaged photon polarizations. The dotted line corresponds to the Born approximation (p^2 order), the dash-and-dot line up to p^4 , the dashed line up to p^6 order. The full line denotes the complete tree order NJL result.

Fig. 1

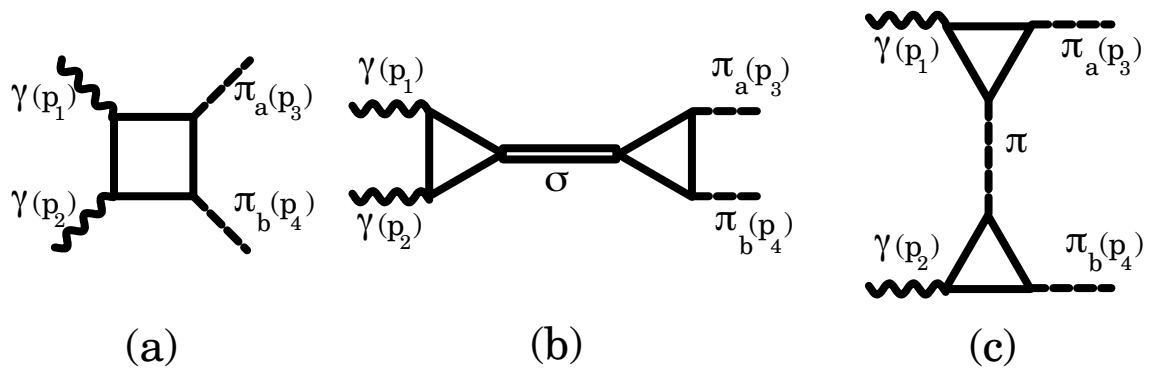


Fig. 2

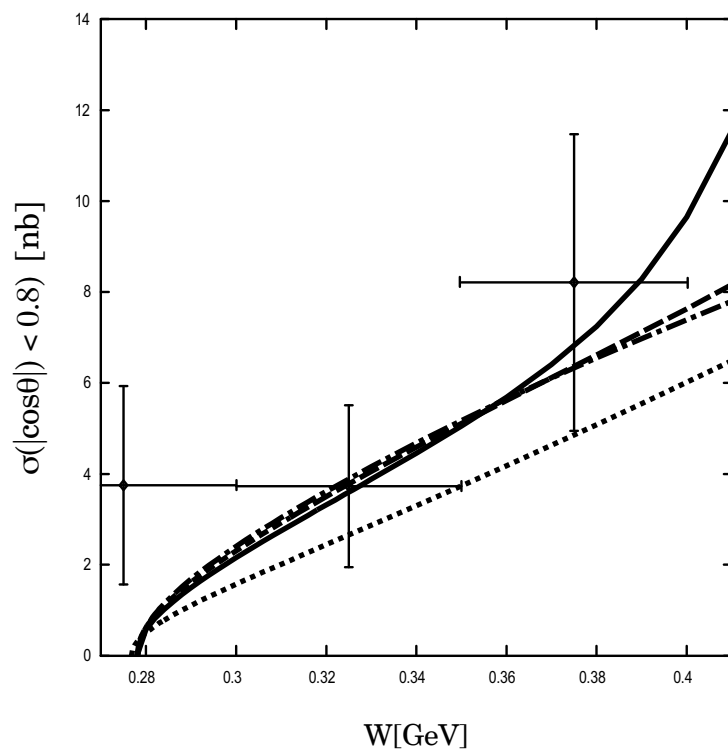
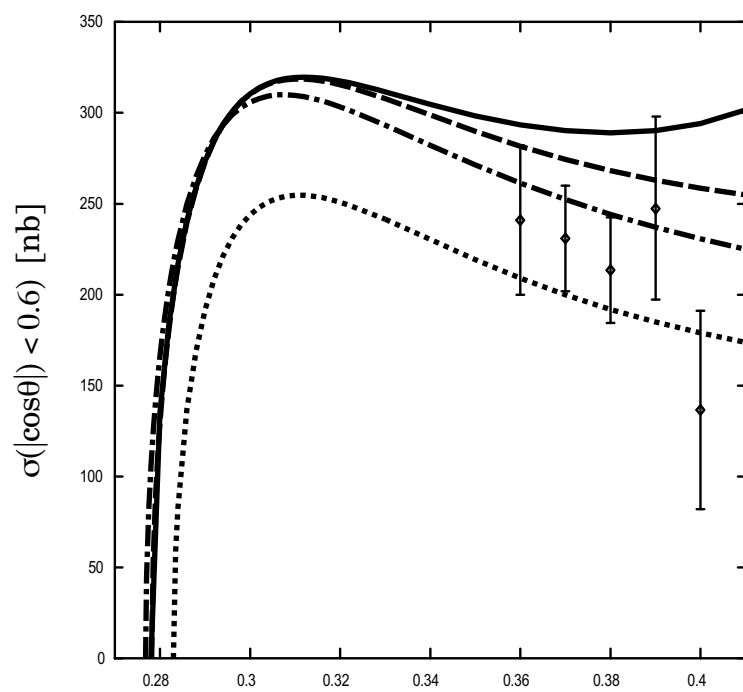


Fig. 3



W[GeV]